ICP-1131

ALTERNATIVE FUEL CYCLE TECHNOLOGY PROGRESS REPORT FOR JULY 1 — SEPTEMBER 30, 1977

October 1977

Allied Chemical
IDAHO CHEMICAL PROGRAMS

IDAHO NATIONAL ENGINEERING LABORATORY

ENERGY RESEARCH AND DEVELOPMENT ADMINISTRATION

IDAHO OPERATIONS OFFICE UNDER CONTRACT EY-76-C-07-1540

Printed in the United States of America
Available from
National Technical Information Service
U.S. Department of Commerce
5285 Port Royal Road
Springfield, Virginia 22161
Price: Printed Copy $4.50; Microfiche $3.00

ICP-1131

UC-78
LWR Technology
TID-4500, R65

ALTERNATIVE FUEL CYCLE TECHNOLOGY

PROGRESS REPORT FOR JULY 1 - SEPTEMBER 30, 1977

Cyril M. Slansky, Editor

Work performed under the direction of:

B. C. Musgrave, Manager
Technical Division

B. R. Dickey, Assistant Manager
Technical Division

K. L. Rohde, Assistant Manager
Technical Division

Date Published - October 1977

ALLIED CHEMICAL CORPORATION
IDAHO CHEMICAL PROGRAMS - OPERATIONS OFFICE

Prepared for

ENERGY RESEARCH DEVELOPMENT ADMINISTRATION
IDAHO OPERATIONS OFFICE
UNDER CONTRACT EY-76-C-07-1540

ABSTRACT

Quarterly progress is reported on alternative fuel cycle technology studies for the Savannah River Laboratory. Off-gas studies are reported on the adsorption of gaseous iodine on silver-exchanged mordenite. Waste management studies include the evaporation and corrosion behavior of simulated high-level liquid waste in a thermosiphon evaporator and engi- studies on a laboratory-size storage tank.

SUMMARY

I. LWR OFF-GAS TREATMENT

The final draft of a report entitled, "NO_x Abatement with Ammonia by Hydrogen Mordenite at Nuclear Reprocessing Plants", has been prepared.

II. IODINE-129 ADSORBENT AND STORAGE DEVELOPMENT

Tests to determine the effects of water vapor, NO and NO_2 on the elemental-iodine (I_2) loading of silver-exchanged mordenite was completed. The highest iodine loadings were obtained with NO in the gas stream. Using simulated dissolver off-gas streams, loadings of about 170 mg I_2/g adsorbent and a decontamination factor of 10^3 to 10^4 were obtained. This represents about 72% conversion of the silver to silver iodide. The data indicate that NO keeps the silver in the metallic state, which has a higher capacity for iodine than the oxide. In the absence of NO, NO_2 appears to slowly oxidize silver to silver oxide, and cause lower iodine loadings. This should not present a problem as the primary NO_x species in dissolver off-gases will be NO. Water vapor appeared to have no effect on the iodine loadings.

Recycle tests on a bed of silver-exchanged mordenite, in which the iodine was repeatedly loaded as I_2 and stripped as hydrogen iodine (HI), were completed. The bed was recycled 13 times. The data indicate a 50% loss in the initial iodine-loading capacity would occur after 18 cycles. The loss in loading capacity is believed due to a slow but progressive pore collapse which blocks access to the silver sites.

Tests to determine the iodine loadings of lead-exchanged zeolites, which were used to chemisorb HI during the recycle tests, were completed. Loadings up to 408 mg HI/g substrate were obtained. This represents about 90% use of the lead to form chemisorbed iodine. The iodine-vapor pressures over the substrates were predicted to be 10^{-6}, 10^{-8} and greater than 10^{-16} atm for lead-exchanged mordenite, lead-exchanged faujasite and reduced lead-exchanged faujasite, respectively. All the above substrates may be suitable for long-term storage of ^{129}I. The topical report covering the information given in this and in the previous quarterly report (ICP-1122) is being prepared.

The iodine adsorbent program will be ended this quarter. Additional work should be done to:

(a) Measure the loading capacity of silver-exchanged mordenite for airborne-organic iodides.

(b) Determine the effects of water vapor, NO and NO_2 on the iodine loadings of silver-exchanged mordenite not pretreated with hydrogen.

(c) Conduct design verification studies on the regeneration and recycle of silver-exchanged mordenite in pilot plant studies.

(d) Search for other silver-loaded substrates that might be more suitable for regeneration and recycle than silver-exchanged mordenite.

(e) Complete the evaluation of recycle life of Ag°Z, i.e., measure the complete life cycle of the adsorbent.

III. LIQUID WASTE MANAGEMENT: EVAPORATION AND STORAGE

The small-scale thermosiphon evaporator was operated successfully with a titanium reboiler tube section for the evporation of both nitric acid and simulated high-level liquid waste (HLLW). The heat transfer coefficients for the titanium reboiler tube with dilute nitric acid were approximately the same as with the Type 304L stainless steel reboiler tube. However, significantly lower heat transfer coefficients were obtained during the evaporation of more concentrated nitric acid and both dilute and concentrated HLLW. The lower heat transfer coefficients are attributed to the buildup of solids on the titanium reboiler tube surface. After 432 hours of operation the titanium reboiler tube had no measurable weight change attributable to corrosion.

The Laboratory Storage Tank was operated with both nitric acid and HLLW. The cooling water coils showed significantly lower heat transfer coefficients for nitric acid and HLLW than for water.

The characteristics of undissolved solids particles in freshly stored HLLW slurries were compared to those of aged slurries and to the scale deposited on the heat transfer surfaces of the small-scale thermosiphon evaporator.

Evaluation of the remote electronic corrosion monitoring techniques continued with a comparison to rates for corrosion coupons in the same solutions.

Laboratory corrosion coupon studies with Type 304L stainless steel indicated that technetium accelerates corrosion in dilute nitric acid, has little effect in HLLW without ruthenium, and inhibits the accelerating effects of ruthenium.

CONTENTS

FIGURES AND TABLES

Figures

Tables

INTRODUCTION

This quarterly report is one of a series reporting progress by Allied Chemical Corporation - Idaho Chemical Programs at INEL on the Alternative Fuel Cycle Technology national programs which are administered by Savannah River Operations, ERDA, and the Savannah River Laboratory. Previous quarterly reports were published as ERDA reports ICP-1101, ICP-1108, ICP-1110, ICP-1116, and ICP-1122.

The studies are identified as:

Off-Gas Treatment:	F-ID-13-001
Waste Management:	F-ID-13-002
^{129}I Adsorbent and Storage Development:	F-ID-13-004

RESULTS

I. LWR OFF-GAS TREATMENT

(R. A. Brown, D. H. Munger, and T. R. Thomas)

The final draft of a report entitled, "NO_x Abatement with Ammonia by Hydrogen Mordenite at Nuclear Reprocessing Plants", has been prepared.

Plans for Next Quarter

The LWR off-gas treatment program will be terminated this quarter. Reactor engineering studies should be made to determine a design equation and product distribution for the above NO_x abatement technology.

II. IODINE-129 ADSORBENT AND STORAGE DEVELOPMENT

(L. P. Murphy, B. A. Staples, and T. R. Thomas)

Tests to determine the effects of water vapor, NO and NO_2 on the iodine loadings of silver-exchanged mordenite Zeolon 900 (AgZ) have been completed. The AgZ was pretreated with H_2 at 500°C for 24 hr to reduce the silver to the metallic state (Ag^oZ) before testing. All loading tests were run in airstreams using the following conditions: bed weight, 270 g; bed depth, 15 cm; bed diameter, 5 cm; superficial face velocity, 15 m/min; bed temperature, 150°C; airborne-elemental iodine concentration, about 1500 mg I_2/m^3; and decontamination factor at breakthrough, 10^3 to 10^4.

The iodine-distribution and -loading data are given in Table 1.

TABLE 1

IODINE LOADING and DISTRIBUTION vs. CONTAMINANT GASES

Test Conditions			mg I_2/g Ag^oZ in each 2.5 cm Segment[b]						
Water Vapor (%)[a]	NO_2 (%)	NO (%)	1	2	3	4	5	6	Avg. Loading (mg I_2/g Ag^oZ)
0	0	0	174	160	141	121	69	15	113
6	0	0	155	136	123	89	35	3	91
0	2	0	97	100	91	73	39	9	68
6	2	0	125	127	119	121	81	17	98
0	0	2	163	171	170	134	93	22	129
6	0	2	169	167	143	123	74	10	115
0	2	2	187	181	185	169	103	21	141
6	2	2	181	172	163	129	65	9	120

[a] Dew point = 35°C

[b] The average value of duplicate or triplicate tests

The data in Table 1 indicate that the first 5 to 7.5 cm of the test beds attain a saturation loading; the distribution of iodine is about constant. The remaining 7.5 cm is in the mass-transfer zone.

In Table 2, the average iodine loadings in the saturation and mass-transfer zones are given.

An analysis of the saturation-zone data based on a three-level factorial design and the 95% confidence interval of an effect indicate:

(a) NO effect = 40 ± 12 mg I_2/g Ag°Z; adding NO to the gas stream enhances the iodine loading.

(b) NO_2 effect = -12 ± 12 mg I_2/g Ag°Z; within the confidence limits of an effect, the negative influence of NO_2 is not clearly established.

TABLE 2

IODINE LOADINGS IN SATURATION AND MASS-TRANSFER ZONES VS CONTAMINANT GASES

Test Conditions			Loadings (mgI_2/g Ag°Z)[a]		
Water Vapor (%)	NO_2 (%)	NO (%)	Saturation Zone[b]	Mass-transfer Zone[c]	Over-all Average
0	0	0	159 ± 17	69 ± 17	113 ± 12
6	0	0	138 ± 17	43 ± 17	91 ± 12
0	2	0	96 ± 17	41 ± 17	68 ± 12
6	2	0	124 ± 17	73 ± 17	98 ± 12
0	0	2	168 ± 14	90 ± 14	129 ± 10
6	0	2	159 ± 17	69 ± 17	115 ± 12
0	2	2	185 ± 14	98 ± 14	141 ± 10
6	2	2	171 ± 17	67 ± 17	119 ± 12

[a] The error limits represent the 95% confidence interval for duplicate or triplicate tests based on a pooled variance.

[b] The average loading on the first three segments in Table 1.

[c] The average loading on the last three segments in Table 1.

(c) H_2O effect = -4 ± 12 mg I_2/g Ag°Z; the presence or absence of water vapor has no significant effect on the iodine loadings.

(d) NO x NO_2 interaction = 25 ± 12 mg I_2/g Ag°Z; the interaction between NO and NO_2 is large; at low levels of NO, the effect of increasing NO_2 is a reduction in loading. At higher NO levels, the NO_2 effect becomes small.

(e) H_2O x NO_2 interaction = 11 ± 12 mg I_2/g Ag°Z; the interaction between water and NO_2 is insignificant.

(f) H_2O x NO = 7.5 ± 12 mg I_2/g Ag°Z: the interaction between water and NO is insignificant.

A similar analysis of the data in the mass-transfer zone and the overall average loading both indicate a large positive effect due to NO. However, no other main effects or interactions were found significant.

A graphical presentation of the effect-test data (Figure 1) illustrates the positive influence of NO on the iodine loadings. In the absence of NO, NO_2 has a negative influence. However, the large NO x NO_2 interaction (i.e., 25 ± 12 mg I_2/g Ag°Z) identified in the three-level factorial designs prevents a clear statistical interpretation of the positive and negative effects of NO and NO_2, respectively.

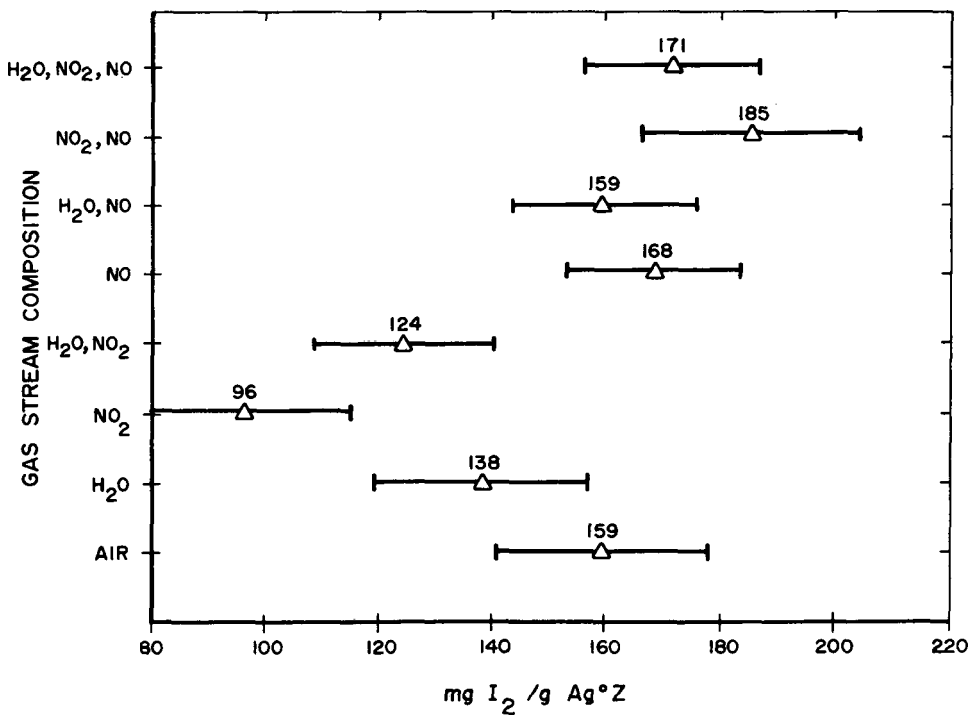

Figure 1. Iodine Loadings in the Saturation Zone of Ag°Z vs Gas Stream Composition

The effects of NO and NO_2 may be due to the equilibrium:

$$2\ Ag°(s) + NO_2(g) \rightleftarrows Ag_2O(s) + NO(g)$$

In the absence of a matrix effect by the mordenite, the free energy of reaction for converting the metal to the oxide would be 6.3 kcal/mole at 150°C. Oxide formation is thermodynamically unfavorable, and could only occur in the absence of NO in the test gas. The presence of NO acts as a reductant to hold the silver in the metallic state even in the presence of $O_2(g)$. AgZ has about half the iodine-loading capacity of Ag°Z (ICP-1122). This result was checked by running a test with AgZ using a test gas containing 2% NO_2 and 6% H_2O at 150°C. The loading was 69 mg I_2/g AgZ, which is about half the value obtained for Ag°Z (124 $\pm$ 17 mg I_2/g Ag°Z in Table 1). In the absence of NO, NO_2 is partially oxidizing the Ag°, and causing lower iodine loadings. The primary NO_x species in the dissolver off-gases of reprocessing plants will be NO. Consequently, the Ag°Z should remain in the reduced state, and the maxium iodine loadings given in Table 2 and Figure 1 should be obtainable. A loading of 170 mg I_2/g Ag°Z represents about 72% conversion of the Ag° to silver iodide.

The recycle of a bed of Ag°Z was continued. The experimental conditions and results of the first five cycles are given in the previous quarterly report (ICP-1122). The test bed has been recycled 13 times; the results of the loading tests, along with the distribution of iodine are given in Table 3.

The iodine loading reaches a maximum on the second cycle. This is attributed to elimination of zeolitic waters and further reduction of silver to the metal during the first three exposures to H_2 at 500°C during regeneration. Beyond the second recycle, reduction in iodine loading is attributed to progressive pore collapse and decreasing accessibility of the silver atoms.

Figure 2 illustrates the iodine loading in the saturation zone vs the number of recycles. A linear least-squares fit of the data was made on the iodine loadings for recycles 2 through 13. Extrapolation of the data indicate a 50% loss in initial iodine-loading capacity would occur by cycle 18.

The amount of iodine that could be stripped with H_2 from the iodine-loaded Ag°Z bed (AgIZ) vs the regeneration cycle is given in Figure 3. The data indicate that complete iodine stripping is obtainable for the first five cycles (the low point on the second cycle resulted from incomplete drying of the test bed before stripping). Beyond the seventh cycle, an additional 16 hr was needed to achieve greater than 90% iodine removal. The increasing resistance to total iodine removal is believed due to diffusion resistance from progressive pore collapse.

During the regeneration tests, the desorbed HI from the AgIZ bed was chemisorbed on lead-exchanged zeolites downstream. The bed temperature was 150°C and the superficial face velocity about 8 m/min. All other

TABLE 3

IODINE LOADING ON Ag°Z VS NUMBER OF RECYCLES

Cycle	mg I_2/g Ag°Z in each 2.5 cm segment						Avg. Loading (mg I_2/g Ag°Z)
	1	2	3	4	5	6	
0	179	174	164	132	60	7	119
1	182	170	161	127	71	10	120
2	212	201	178	147	76	13	138
3	192	192	180	150	70	5	131
4	194	189	179	145	67	8	130
5	191	180	176	147	80	10	131
6	169	166	154	142	94	21	124
7	188	174	169	139	61	12	124
8	165	182	158	142	47	8	117
9	137	129	125	88	46	11	89
10	149	143	128	103	42	6	95
11	141	117	154	85	95	36	105
12	137	130	129	114	70	18	100
13	143	140	131	107	51	13	98

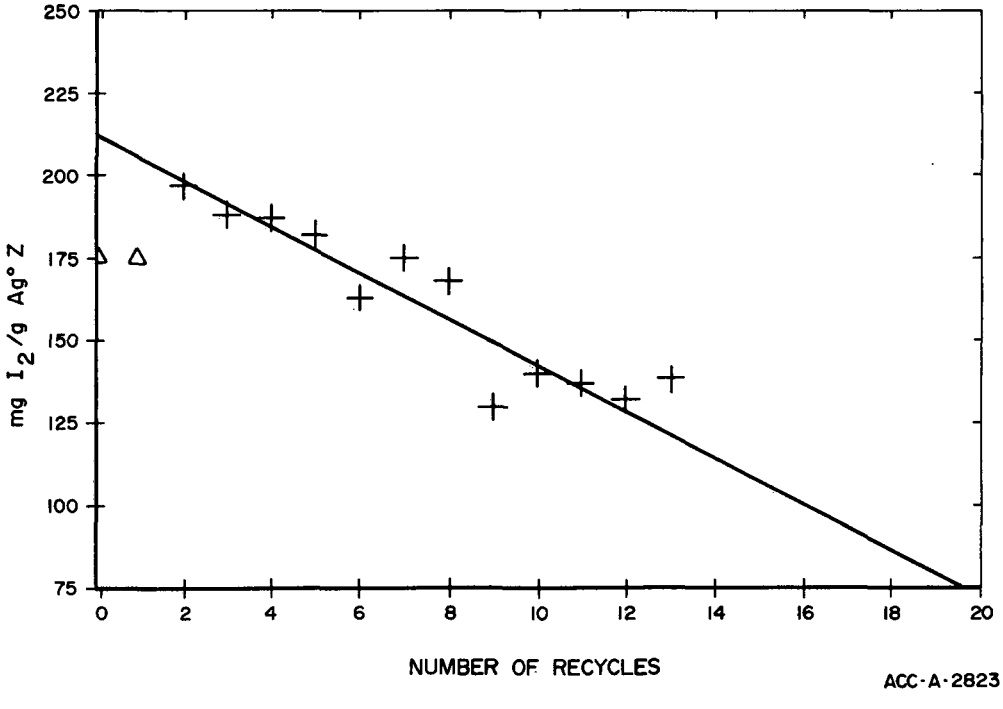

Figure 2. Iodine Loadings of Recycled Ag°Z

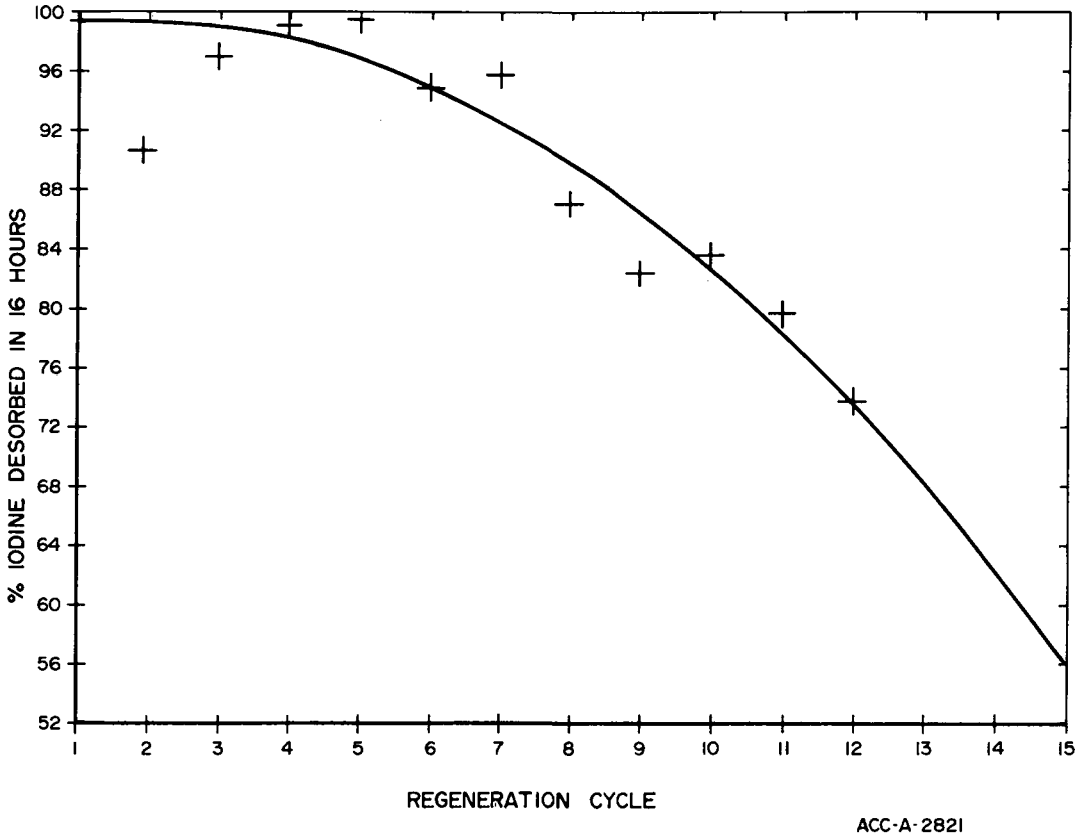

Figure 3. Iodine Desorbed vs Regeneration Cycle of AgIZ

test conditions were identical to those given for iodine stripping of the AgIZ bed (see Table 1 in the previous quarterly, ICP-1122). Table 4 gives the results of the loading tests.

TABLE 4

HYDROGEN IODIDE LOADINGS ON LEAD-EXCHANGED ZEOLITES IN DRY HYDROGEN AT 150°C

Zeolite	No. of Tests	Iodide Loadings (mg HI/g Zeolite) Average	Range
PbX[a]	5	408 ± 22[d]	378-436
$Pb^{0}X$[b]	1	192	-
PbZ[c]	2	380	361-398

[a] Lead-exchanged faujasite

[b] PbX exposed to H_2 at 500°C for 24 hr

[c] Lead-exchanged mordenite

[d] The 95% confidence interval of the average

The data indicate that the best loadings are obtained on PbX and about 90% of the lead is being used to chemisorb HI.

Tests were completed to determine the vapor pressures of iodine chemisorbed in PbX, $Pb^{O}X$ and PbZ (PbIX, $Pb^{O}IX$, and PbIZ, respectively). Solid samples were placed in a heated optical cell and the vapor pressure of $I_2(g)$ vs temperature determined from the absorption intensity of the $I_2(g)$ visible spectrum. The data were fitted by least squares to the equation:

$$\ln P_{I_2} = A + B/T$$

where P = the vapor pressure of elemental iodine and T is in K. The values of A and B for the substrates and the predicted value of P_{I_2} at 20°C by extrapolation are given in Table 5.

TABLE 5

IODINE VAPOR PRESSURE DATA FOR CHEMISORBED IODINE ON LEAD-EXCHANGED ZEOLITES

Substrate	Gas Blanket	A	B	P_{I_2} at 20°C (atm)
PbIX	Air	15.3	9.47×10^{3}	4.0×10^{-8}
	Nitrogen	17.3	1.01×10^{4}	3.4×10^{-8}
$Pb^{O}IX$	Air	44.5	2.65×10^{4}	9.5×10^{-21}
	Nitrogen	51.6	3.02×10^{4}	2.3×10^{-16}
PbIZ	Air	6.6	5.53×10^{3}	4.4×10^{-6}
	Nitrogen	8.0	6.20×10^{3}	1.8×10^{-6}

The above extrapolated vapor pressures are related to the strength of the lead-iodine bond. Pure PbI_2 has an iodine-vapor pressure of about 10^{-28} atm at 20°C. The chemisorbed bonds are considerably weaker than the iodide bond. However, the iodine-vapor pressures may be small enough that all the above listed substrates would be suitable for long-term storage of ^{129}I in sealed containers at ambient temperatures.

A mass-balance test was run to determine if $I_2(g)$ were the only significant iodine species that would desorb from PbIX. A gas stream of nitrogen was passed through the optical cell containing the PbIX at 175°C for 16 hr. The absorbance of the $I_2(g)$ was monitored continuously. The iodine desorbed from the PbIX was calculated by graphical integration of the equation:

$$\text{mg } I_2(g) = \frac{f \cdot m}{a \cdot b} \int_0^t \text{Abs} \cdot dt$$

where Abs = the observed absorbance, t = time in hr, f = nitrogen flow

rate in cm^3/hr, m=254 mg $I_2/22.4\ cm^3$, a = the molar absorbtivity of iodine (18.54 atm^{-1} at 520 nanometers, and b = the path length of the cell (10 cm). The weight of iodine desorbed as determined by the above equation was compared to the gravimetric weight loss on the PbIX. The two methods gave a weight loss within 10% of each other which indicates the primary, if not the sole volatile species to be $I_2(g)$.

Plans for Next Quarter

The iodine-129 adsorbent and storage program will be terminated this quarter. The first draft of a topical report covering the information in this and the previous quarterly report (ICP-1122) is being prepared. The final draft will be completed in October 1977.

Based on the results of this program, the following work should be done:

(1) Study the loading capacity of Ag°Z for airborne-organic iodides

(2) Determine the effect of water vapor, NO and NO_2 on the iodine loadings of AgZ.

(3) Conduct design verification studies on the regeneration and recycle of Ag°Z in pilot-plant studies.

(4) Search for other silver-loaded substrates that might be more suitable for regeneration and recycle than Ag°Z.

(5) Complete the evaluation of recycle life of Ag°Z, i.e., measure the complete life cycle of the adsorbent.

III. LIQUID WASTE MANAGEMENT: EVAPORATION AND STORAGE[a]

(B. E. Paige, P. A. Anderson)

The reprocessing of spent nuclear fuel by several of the presently considered alternative fuel cycles generates liquid wastes which must be stored for short or intermediate periods pending solidification. The liquid storage capacity of waste tanks can be reduced and more efficiently utilized if the waste is concentrated to the smallest practical volume before and/or during storage.

The present studies are concerned with the nitric acid wastes which result from the tributyl phosphate extraction of uranium. Simulated solutions are used to avoid the difficulties and expense of experimenting with actual radioactive solutions. The objectives are to investigate the quantities and nature of the undissolved solids and materials of construction for process operating conditions during the concentration and storage of high-level liquid wastes (HLLW).

Factors being investigated include the effects of solids deposition on heat transfer surfaces in two separate phases of processing: (1) the thermosiphon evaporation of dilute HLLW and (2) the interim storage

[a]Part of the Alternative Fuel Cycle Technology program administered by Savannah River Operations and Savannah River Laboratory.

of concentrated HLLW during which fission product heat is removed by cooling-water coils. Data from earlier laboratory investigations in both of these areas,[1] in addition to data on the physical properties of evaporated HLLW,[2] provided the bases for the design of the present experimental equipment and the selection of physical and chemical properties to be studied. Evaluation of the corrosive effects of individual and combined species in liquid wastes are continuing.

1. Evaporation

The small-scale thermosiphon evaporator was operated this quarter with a titanium reboiler tube using nitric acid and simulated HLLW solutions as was done during the previous quarter with the Type 304L stainless steel specimen.[1] The evaporator unit is constructed of Type 304L stainless steel; only the reboiler tube sections are changed as subsequent alloys are tested. The two levels of evaporation which were selected were 340 L/MTU (90 gal/MTU) and 1380 L/MTU (365 gal/MTU). Based upon earlier laboratory evaporation of HLLW, 340 L/MTU represents the upper practical concentration limit from the standpoint of total solids content. A concentration of 1380 L/MTU was selected as a lower concentration limit for short-term cooled fuels and also allows for the possibility of considerable in-tank concentrating during interim storage. Based on these limits, runs were made under the following operating conditions:

(1) The continuous evaporation of solution from 4900 L/MTU containing 2.5 M nitric acid to 1380 L/MTU containing 7 M nitric acid for 48 h.

(2) The continuous evaporation of reconstituted solutions from run (1) from 4900 L/MTU containing 2.5 M nitric acid to 340 L/MTU containing 7 M nitric acid at vapor velocities of 0.3 and 0.6 m/s (1 and 2 ft/s) for 68 h.

  (2a) The recirculation of the solution from run (2) at 340 L/MTU for an additional 48 h while recycling all condensate.

(3) The continuous evaporation of reconstituted solution from run (2) from 4900 L/MTU containing 2.5 M nitric acid to 340 L/MTU containing 7 M nitric acid at vapor velocities of 0.9 and 1.2 m/s (3 and 4 ft/s) for 52 h.

A complete set of runs was first made with nitric acid to establish a baseline for the titanium reboiler tube material. The runs were then repeated under the same operating conditions using simulated HLLW solution.

---

[1] Alternative Fuel Cycle Technology Progress Report for April 1 - June 20, 1977, ICP-1122 (April 1977).

[2] LWR Fuel Reprocessing and Recycle Progress Report for January 1 - March 31, ICP-1116 (April 1977).

The HLLW feed contained 6 g/L total fission products which represent extraction raffinate at 4900 L/MTU from fuel irradiated to 33,000 MWd/MTU and cooled for 150 days. The HLLW feed also contained 2 g/L uranium, 7 g/L gadolinium, 0.34 g/L phosphate and 0.01 g/L dissolved corrosion products.[2]

To minimize the time required to obtain steady state operating conditions, the evaporator was charged with HLLW which was already adjusted to the expected concentration of the evaporator product.

1.1 Operating Characteristics of Evaporator (G. R. Villemez, C. B. Millet)

Plugging problems which were previously experienced with the settling of undissolved solids in concentrated HLLW (340 L/MTU) were eliminated with the removal of the preheater. An automatic control valve was installed in the feed line, eliminating the previous problem of unstable operating conditions.[1]

The maximum waste solution temperature allowed in the waste evaporator is 130°C due to the explosion hazard of tributyle phosphate and nitric acid above 140°C.[3] The evaporator can be operated with a throughput of 300 to 1200 g/h of vapor condensate consisting of approximately 2 M nitric acid. This corresponds to a vapor velocity range of 0.3 to 1.22 m/s (1 to 4 ft/s).

1.2 Heat Transfer of Evaporator (G. R. Villemez, C. B. Millet)

The heat transfer for the titanium reboiler tube was calculated on the same basis as the Type 304L stainless steel reboiler tube.[1] The rate of heat transfer (q), is defined as the product of the overall heat transfer coefficient (U), the area of heat transfer surface (A), and the apparent temperature difference (ΔT). The heat transfer expression is:

$$q = U \cdot A \cdot \Delta T$$

The rate of heat transfer, q, was calculated as the product of the vapor rate at the atmospheric pressure of 84.7 kPa (12.3 psi) at 1585 metres (5200 ft) elevation and the latent heat of the evaporation of water at the saturated vapor temperature. The area is based on the inside diameter of a 1-inch reboiler tube with 30 cm (12 in.) of reboiler tube exposed to condensing steam; an additional 7.5 cm (3 in.) portion of the reboiler tube was exposed to the steam condensate. The feed solution was preheated by the steam condensate to the temperature of the recirculated solution, which was near the boiling point at the feed end for the reboiler section. The apparent temperature difference was calculated from the measured saturated vapor temperature above the boiling liquid and the condensing steam temperature. The calculated heat transfer rates are estimated to be within 10% of the actual value.

---

[3]Hanford Atomic Products Operation, Purex Technical Manual, HW-31000 DEL. March 25, 1955, Part III, p 1007.

1.21 Rate

The apparent overall heat transfer coefficeints with the titanium reboiler tube were calculated from operating data obtained during steady state conditions.[1] Data from the first nitric acid evaporation to 1380 L/MTU indicated little, if any, effect on the heat transfer coefficients from solids formation in the titanium reboiler tube. However, the solids buildup appeared to reduce the heat transfer coefficients during runs with the nitric acid to 340 L/MTU. The overall heat transfer coefficients for titanium were approximately 55% of the values for Type 304L stainless steel in the nitric acid solutions evaporated to 340 L/MTU. These data are shown in Figure 4.

The heat transfer coefficients for titanium during the evaporation of the HLLW solutions to 340 L/MTU were essentially the same as the baseline nitric acid values at this concentration. The overall heat transfer coefficients for titanium were 65 to 95% of the values for Type 304L stainless steel in HLLW solutions evaporated to 340 L/MTU as shown in Figure 5.

As shown in Figures 4 and 5, the overall heat transfer coefficients increased with an increase in the vapor velocity but decreased with the accumulation of operating time on the titanium reboiler tube. The decreased values in the second and third evaporation runs are apparently due to scaling effect.

Even though the scale deposition appeared to continuously reduce the overall heat transfer coefficient during evaporation, the titanium material is preferable to Type 304L stainless steel due to its superior corrosion resistance as reported in Section 3.2.

1.22 Scaling and Fouling

Solids were formed in the titanium reboiler tube section during the evaporation of 7 M nitric acid. The solids which deposited on the feed end of the reboiler tube are shown in Figure 6, and those which deposited on the tube sheet are shown in Figure 7.

The loose dark gray scale which formed on the surface of the titanium reboiler tube section during the evaporation of nitric acid, contained major amounts of iron and silicon and minor amounts of nickel and chromium. This scale has not formed on either the Type 304L stainless steel reboiler rube or the Nitronic-50 reboiler tube currently being tested. Since all waste solutions contain some stainless steel corrosion products from the process, a plating out of these materials may be the cause of poor heat transfer which has been observed in all titanium evaporators.[4]

The scale which formed in the feed end of the reboiler tube section

[4]M. W. Wilding and B. E. Paige, Survey on Corrosion of Metals and Alloys in Solutions Containing Nitric Acid, ICP-1107 (December 1976).

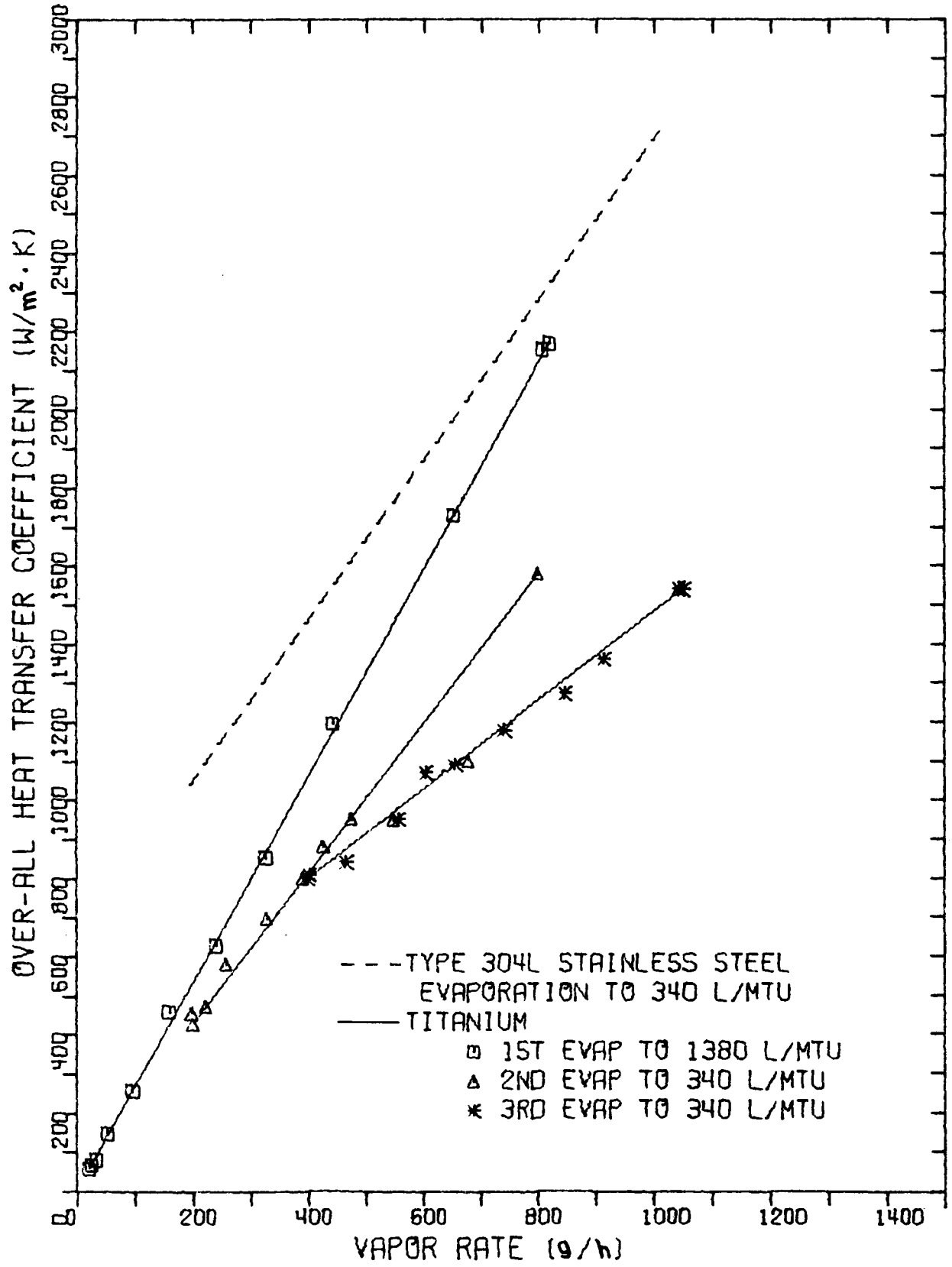

Figure 4. Heat Transfer for a Titanium Reboiler Tube in Nitric Acid

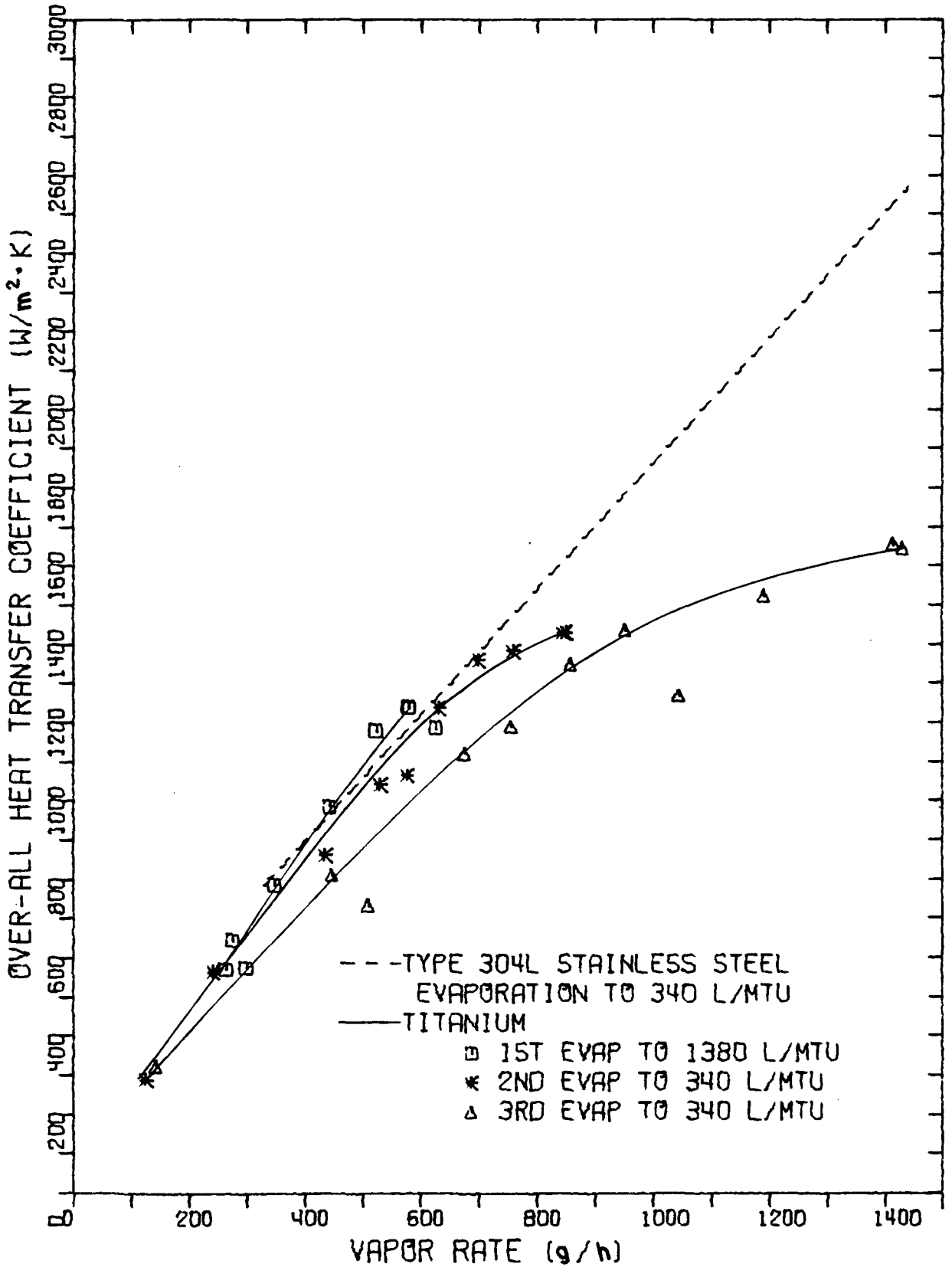

Figure 5. Heat Transfer for a Titanium Reboiler Tube in HLLW

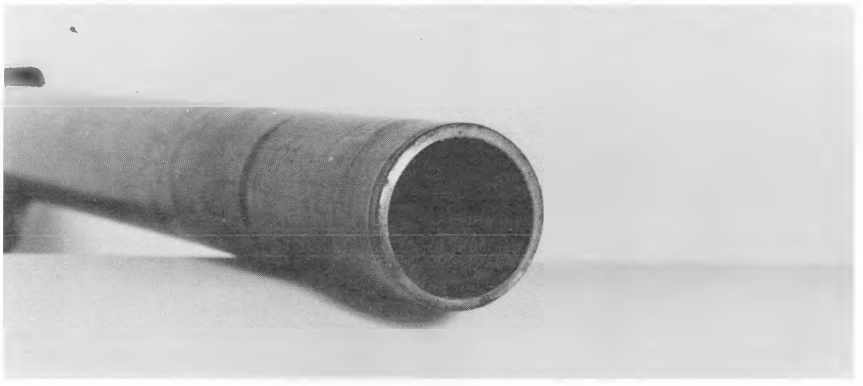

TITANIUM REBOILER TUBE EXPOSED TO
7-MOLAR NITRIC ACID

Figure 6. Solids on Feed End of Reboiler Tube

TITANIUM REBOILER TUBE EXPOSED TO
7-MOLAR NITRIC ACID

Figure 7. Solids on Top End of Reboiler Tube

during the evaporation of the simulated HLLW solution, shown in Figure 8, is a hard thin layer which appears to build up with operating time. The scale deposit was thicker on the tube sheet, shown in Figure 9, than on the feed end. Since these scales continuously reduce the overall heat transfer coefficient during the evaporation, long-term operation may require periodic scale removal processes to maintain an adequate heat transfer rate in the titanium reboiler tubes. Most of the scale from the tube surface was removed after a 6-hour treatment with boiling 10% Turco Alkaline Rust Remover.[a] However, some scale was still visible in the heat transfer area even after scrubbing with a nylon brush.

The scale formed in the titanium reboiler tube section during the evaporation of HLLW consisted mostly of zirconium and molybdenum with traces of iron, which is essentially the same scale formed during previous evaporations of HLLW with a Type 304L stainless steel reboiler tube section. HLLW scale is compared to precipitates from laboratory evaporations in Section 2.23.

2. Waste Storage

The present storage studies with simulated HLLW are designed to provide design and operational data for the safe and economical storage of evaporated liquid wastes pending solidification. The data obtained will be applicable to a variety of types of HLLW's anticipated from any of several possible alternative fuel cycles, including existing defense wastes.

During this quarter, the major effort was directed toward operating the Laboratory Storage Tank, continuation of long-term stability studies with stored HLLW slurries, and further characterization of precipitated solids.

2.1 Laboratory Storage Tank (P. A. Anderson)

Long-term storage studies have been initiated in the Laboratory Storage Tank to obtain preliminary data on heat transfer, mixing, and chemical stability of stored HLLW. Experience with experimental equipment will be utilized in the design and construction of a small-scale storage tank. The tank has been operated with water,[1] 12.8 M nitric acid, and HLLW with a composition representative of waste from an LWR reprocessing plant. A nitric acid concentration of 12.8 M was initially selected because laboratory batch evaporations yielded slurries with this acidity. Recent experience with the small-scale thermosiphon evaporator indicates that 7 M is a more likely acidity for concentrated HLLW slurries. The HLLW slurry which is presently stored is the adjusted product from the small-scale thermosiphon evaporator.

2.11 Heat Transfer

Heat transfer coefficeints at various flowrates of cooling water for stored water, 12.8 M nitric acid, and HLLW at 1380 L/MTU in

[a]Turco Products, Inc., Division of Purex Corporation, Carson, California.

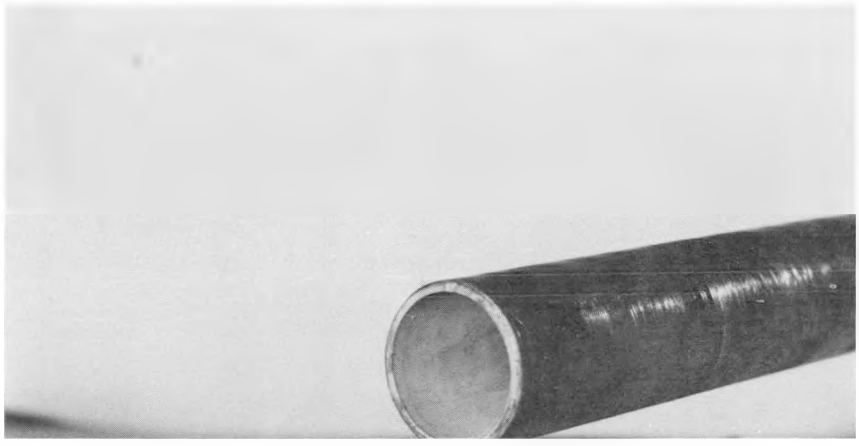

TITANIUM REBOILER TUBE EXPOSED TO LWR WASTE SOLUTION

Figure 8. Scale on Feed End of Reboiler Tube

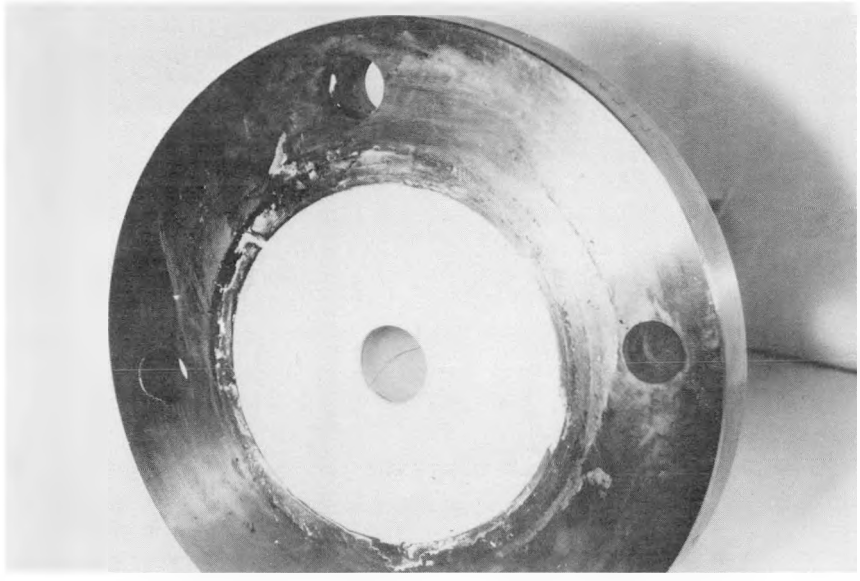

TITANIUM REBOILER TUBE SHEET EXPOSED TO LWR WASTE SOLUTION

Figure 9. Scale on Tube Sheet of Reboiler Tube

5.3 M HNO_3 are shown in Figure 10. Measurements were made while the solutions were thoroughly mixed for uniform temperatures throughout the stored solutions. The cooling water flow through the Type 304L stainless steel cooling coil is entirely in the laminar flow region. The initial heat transfer coefficients for both the nitric acid and the HLLW were substantially lower than for water at nominal storage conditions. In all three cases, measurements were made after the solution was in the tank for only a few days. Future heat transfer measurements will determine effects due to scaling on the heat transfer surfaces during long-term storage at 60°C.

2.12 Physical Mixing of Stored Slurries

The present experimental equipment was designed to agitate the stored solution in a manner which duplicates the conditions in a large storage tank.[1] One selected parameter is a ballast tank nozzle exhaust velocity of 18 m/s. The ballast tank agitators and convection currents provide vigorous agitation for the lower one third of the 13.6-litre tank, decreasing to only gentle circulation at the top. Temperature gradients of 2 to 4°C are observed within the storage tank at the nominal storage temperature of 60°C after only a few minutes of operation when no other form of mixing is applied. Uniform temperatures throughout the tank were obtained only with auxiliary mixing from the airlift circulators. The ballast tank agitators effectively suspend the undissolved solids near the exhaust nozzle; however, those solids on the tank floor opposite the ballast tank nozzles are not entirely dislodged. This indicates that the ballast tank nozzles must be situated to sweep as much of the tank floor as possible.

2.2 Storage of Evaporated HLLW (P. A. Anderson)

During this quarter, the investigation of the stability of stored slurries with respect to quantities of undissolved solids was continued with HLLW solutions containing a wide variety of process additives. X-ray fluorescence, X-ray diffraction, and scanning electron microscope (SEM) techniques were used to compare the undissolved solids from laboratory evaporated slurries and the scale which plated on heat transfer surfaces of small-scale thermosiphon evaporator. The effects of nitric acid and water rinsing upon the solids were also studied.

2.21 Stability of Stored HLLW Slurries

Simulated HLLW slurries from laboratory evaporations have been stored up to 13 months at constant temperatures and without agitation. The data from 18 samples, which were obtained at intervals of one to two months, show no significant changes with respect to quantities of undissolved solids. The storage of these slurries will continue with future analyses made at six-month intervals.

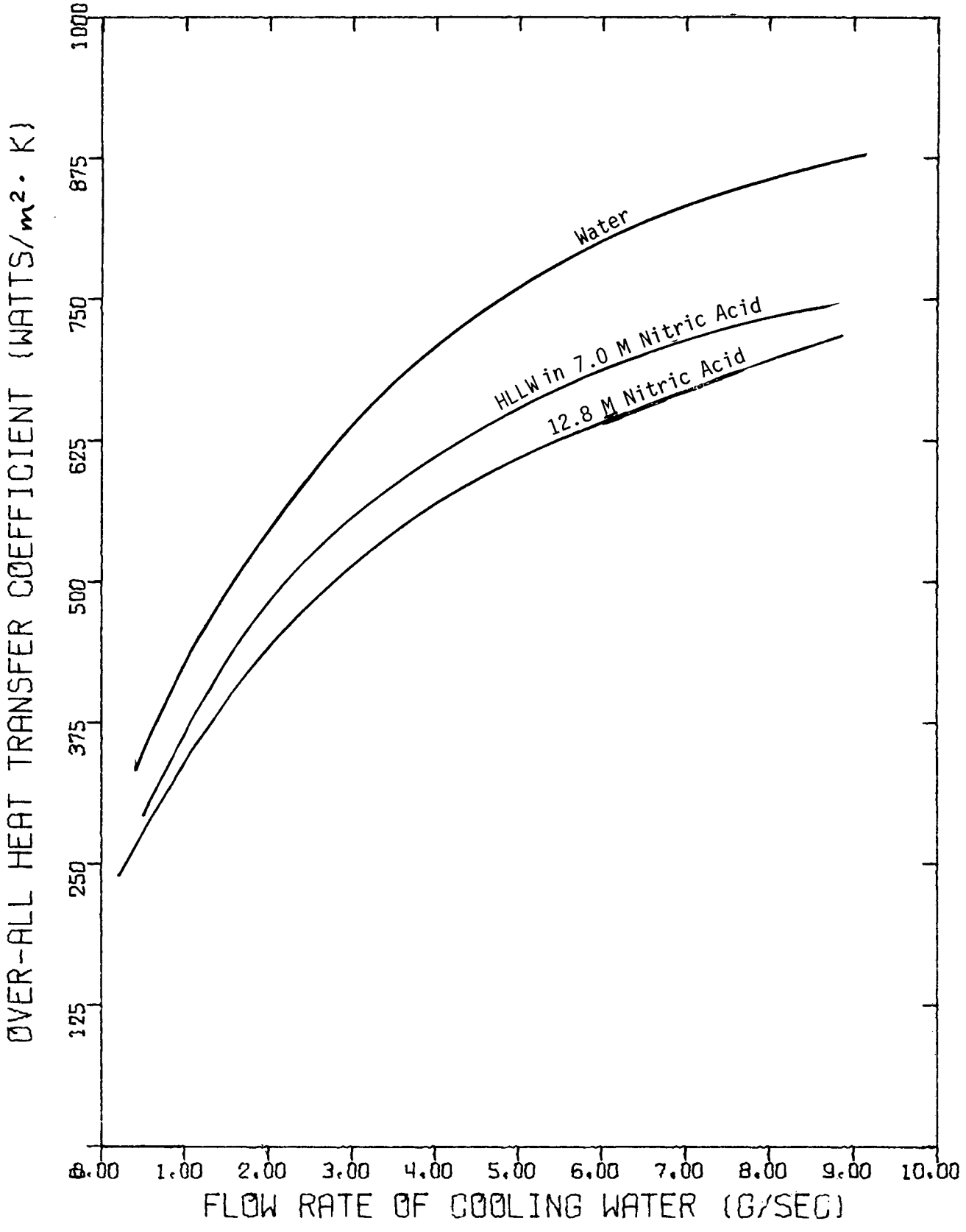

Figure 10. Heat Transfer Coefficients for Cooling of the Laboratory Storage Tank

2.22 Characteristics of the Undissolved Solids in Stored HLLW Slurries

The quantities of total undissolved solids reported[2,5,6] in evaporated HLLW slurries have been based upon analyses in which the filtered solids were not rinsed because of the possibility that rinsing would be likely to dissolve a portion of the solids. X-ray fluorescence and X-ray diffraction data show that thorough rinsing of HLLW solids with water and dilute nitric acid does not alter the chemical composition or the crystalline structure of the particles. Total undissolved solids analyses will continue with the non-rinsing technique.

The solids from a HLLW slurry, which contains 12.8 M nitric acid, 67 g/L gadolinium as a nuclear poison, 0.005 M phosphate, and 0.125 M uranium to simulate total actinides, were examined with a scanning electron microscope (SEM). The precipitate from the slurry when freshly stored, shown in Figure 11, contains cubic particles with a definite crystalline structure. After two months storage at 60°C without agitation, precipitate from the same slurry, illustrated in Figure 12, shows a coating on the particles. Precipitate from the same solution, after three additional months of storage, was thoroughly rinsed with dilute nitric acid and water before SEM examination. Some of the coating material, shown in Figure 13, was still present. Coating effects were not observed after eight months of storage in the non-crystalline particles precipitated from HLLW-0 in previously reported studies.[7] X-ray fluorescence and X-ray diffraction analyses detected no differences in the compositions and crystalline structures of solids due to either the rinsing or the coating material.

The undissolved solids which settle to the bottom of a stored HLLW slurry can be easily resuspended with gentle agitation every few days. Slurries which stand for several months without agitation require more vigorous agitation to resuspend the solids. This indicates that continuous agitation in an actual HLLW storage tank should help prevent caking on the tank floor.

2.23 Comparison of Precipitates and Evaporator Scale

The precipitates from laboratory evaporated HLLW were compared to the scale which formed on the Type 304L stainless steel reboiler tube of the small-scale thermosiphon evaporator during operation with HLLW. Analyses by X-ray diffraction and X-ray fluorescence showed the chemical compositions to be essentially identical except for small amounts of

---

[5] LWR Fuel Reprocessing and Recycle Progress Report for April 1 - June 30, 1976, ICP-1101 (November 1976)

[6] LWR Fuel Reprocessing and Recycle Progress Report for July 1 - September 30, 1976, ICP-1108 (December 1976)

[7] LWR Fuel Reprocessing and Recycle Progress Report for October 1- December 31, 1976, ICP-1110 (January 1977)

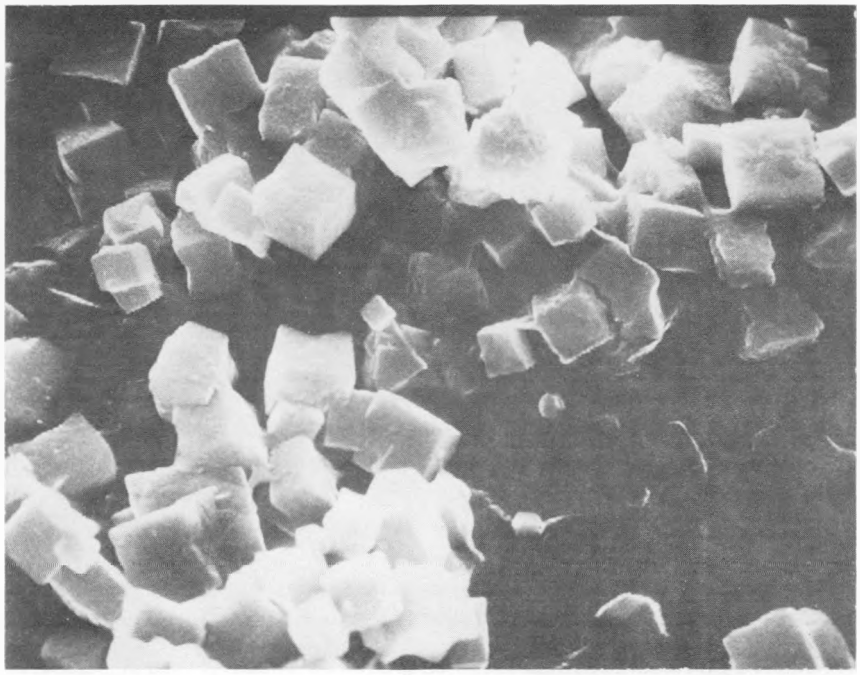

Figure 11. Precipitate from Freshly Stored HLLW
(scanning electron microscope at 5000X magnification)

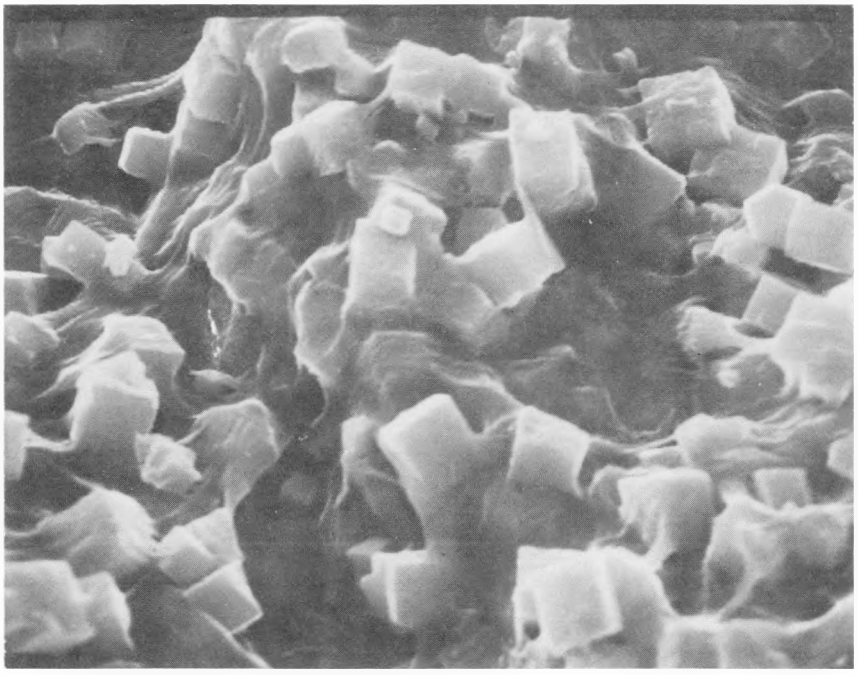

Figure 12. Precipitate from HLLW after Two Months Storage
(scanning electron microscope at 5000X magnification)

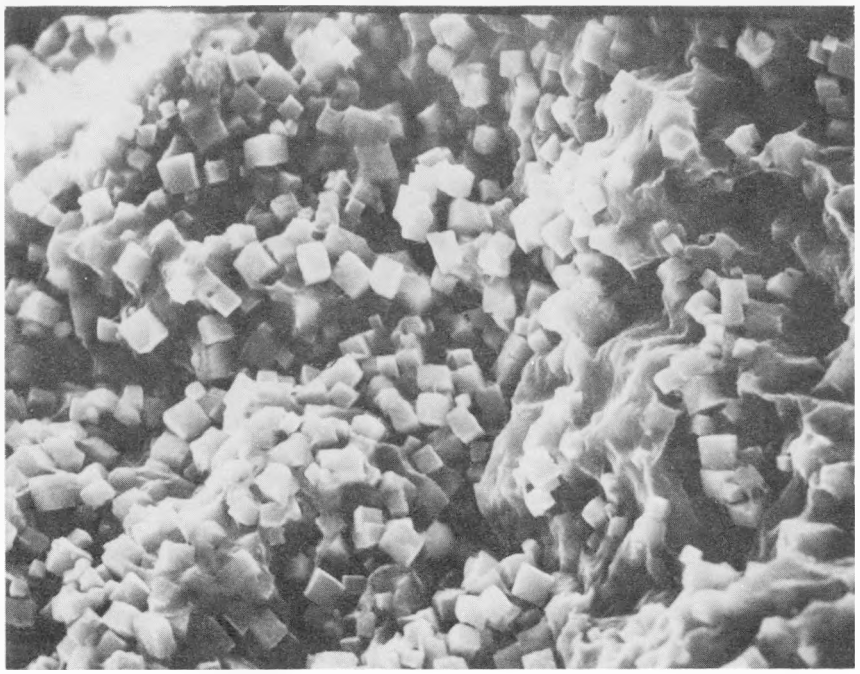

Figure 13. Rinsed Precipitate from HLLW after Five Months Storage
(scanning electron microscope at 5000X magnification)

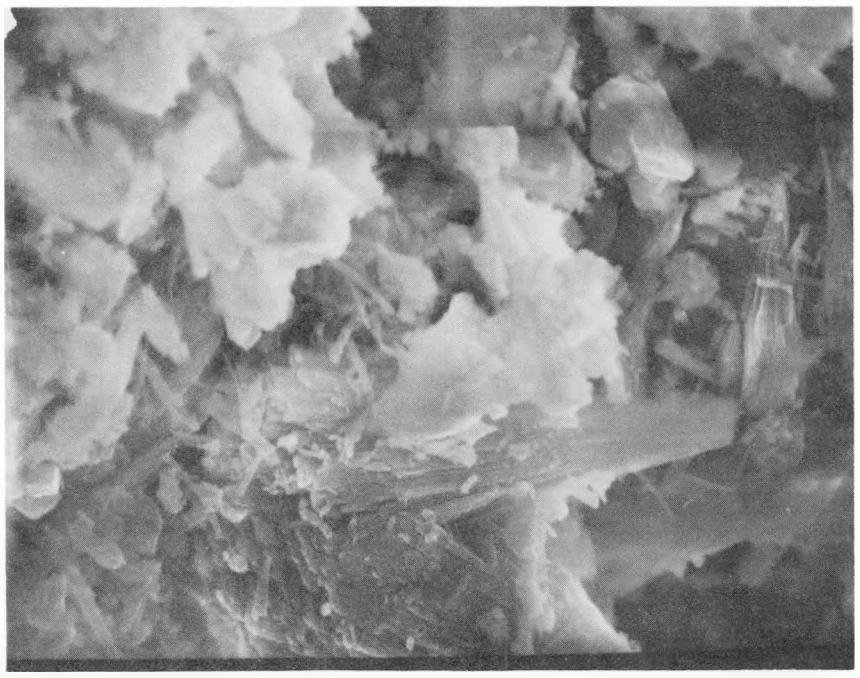

Figure 14. Scale Deposited on Type 304L Stainless Steel
Reboiler Tube during Evaporation of HLLW
(scanning electron microscope at 5000X magnification)

$Fe(UO_2)_2(PO_4)_2 \cdot nH_2O$ which have appeared in the evaporator scale. However, scanning electron microscope examination of the scale, shown in Figure 14, does not indicate the presence of any definite crystalline structure or regular shape of particles as have been found in all of the precipitates which have been examined from laboratory evaporations.

2.3 Design of Small-scale Storage Tank (P. A. Anderson)

A small-scale storage tank is being designed for HLLW storage studies with advanced simulated waste slurries. The tank is being designed for possible application to studies with actual waste solutions generated from hot cell dissolution of irradiated fuels. Improved solution heating will be obtained by stratified heating coils to simulate fission product heat generation differences from suspended and settled components. Solution mixing will be accomplished with ballast tank agitators and thermal convection currents. Water flow in the cooling coils will be in the turbulent range. Type 304L stainless steel will be used as much as possible for the construction of components which contact the stored solutions. The tank will be installed adjacent to the small-scale thermosiphon evaporator and will be filled with evaporator product.

3. Materials and Corrosion

Materials and corrosion studies are being conducted with simulated HLLW slurries in the laboratory and in the small-scale thermosiphon evaporator. The corrosive effects of waste solutions on materials of construction for evaporators, waste tanks, and auxiliary equipment are being studied to identify suitable alloys for fuel reprocessing facilities. Methods for monitoring corrosion of tanks and internal components during interim storage of liquid wastes are being evaluated.

3.1 Monitoring Storage Tanks (P. A. Anderson)

Studies are continuing to evaluate the dependability and accuracy of electronic corrosion monitoring probes in waste tanks and lines. Corrosion monitoring probes, which are constructed of the test alloys, are continuously exposed to the environment being monitored. They are activated weekly, or when desired, to determine accumulated amounts of corrosion. Electronic probes offer the advantage of rapidly obtaining corrosion rate data by remote operation.

Separate Type 304L stainless steel probes were exposed for one to three months to HLLW and 12.8 M nitric acid at 60°C with gentle agitation for one minute each hour to simulate ballast tank mixing in an actual waste tank. A probe was also exposed for one month to HLLW at 1380 L/MTU in 5.3 M nitric acid in the Laboratory Storage Tank. During the three month test period, the electronic equipment indicated continuous corrosion at relatively steady rates. The equipment has operated within the manufacturer's limits of accuracy for the instruments. The corrosion rates indicated by the electronic probes are compared in Table 6 to the rates determined by individual corrosion coupons in the same test solutions.

TABLE 6

CORROSION RATES FOR TYPE 304L STAINLESS STEEL AT 60°C

Type of solution	Corrosion rates from the electronic probes, μm/yr[a]	Corrosion rates from coupons, μm/yr
HLLW at 1380 L/MTU in 7.0 M HNO_3	32	14
HLLW at 1380 L/MTU in 5.3 M HNO_3 with substitutes for Rh, Pd, Tc, and no Ru	8	6.4
12.8 M HNO_3	10.5	10

(a) 1 μm/yr is equivalent to 3.9×10^{-2} mils/yr

These data show that the corrosion rates obtained with the electronic probes are very low and are comparable to the rates determined by corrosion coupons. This is consistent with previous tests in three selected types of HLLW slurries.[2] The evaluation of the performance of electronic corrosion monitoring equipment under simulated process conditions is continuing.

3.2 Reboiler Tube Evaluation (G. R. Villemez, C. B. Millet)

The entire lengths of reboiler tube sections in the small-scale thermosiphon evaporator are used as corrosion specimens. The corrosion rate of the titanium reboiler tube during 432 hours of evaporative service was essentially zero.

3.3 Laboratory Corrosion Tests (C. B. Millet)

Modified Huey tests are being used to determine the corrosion effects of chemical species which are present in actual waste but are not present in simulated waste solutions. Loss of weight by corrosion coupons is determined for three 24-hour periods and one 96-hour period to complete one week of total exposure. Unwelded coupons are submerged in solutions for weight loss measurements and welded coupons are suspended at the vapor-liquid interface to observe weld behavior and possible preferential attack at the interface or in the vapor phase.

Laboratory corrosion tests were performed to determine the effect of the radioactive fission product technetium. Technetium exists only as a radioactive isotope and requires special handling; therefore, it has previously been simulated in HLLW by rhenium or manganese. Technetium

is a corrosion inhibitor for iron and carbon steel,[8] but rhenium does not have a similar effect. Oxidized manganese (Mn[VII]) can be a corrosion accelerator.[9] Since technetium provides inhibition by forming a protective coating, it was not anticipated that it would further protect stainless steel which is already protected by a passive oxide coating.

Three solutions containing technetium at 2.18 g/L, which represents HLLW at 378 L/MTU (100 gal/MTU), were tested at the boiling point on Type 304L stainless steel. The first solution, 7 M nitric acid containing technetium, was found to be nearly twice as corrosive as a pure nitric acid solution. In the second solution, HLLW without ruthenium, the corrosion rate was decreased slightly in the first periods of the test, but by the end of the test, the rate was equivalent to the rate (210 μm/yr) found in previous tests without ruthenium. Overall, the presence of technetium did not change the corrosion rate in HLLW with ruthenium omitted. In the third solution, HLLW containing ruthenium, the corrosion accelerating effects of ruthenium[7,10] were nullified by the technetium. The average corrosion rate (208 μm/yr) was the same as if both ruthenium and technetium had not been present. The observed corrosion in all three tests was general attack in the liquid phase with no preferential vapor phase or interface attack.

The technetium metal dissolved in nitric acid yielded a dark brown solution. At the beginning of these tests, all three solutions were dark brown from the addition of technetium. After boiling for thirty minutes the 7 M nitric acid and the HLLW solution without ruthenium returned to their original color. The color change indicated an oxidation-reduction reaction involving technetium which inhibits valences ranging from seven to zero.[11] The color change was either masked or did not occur in the solution containing ruthenium.

Plans for Next Quarter

The small-scale thermosiphon evaporator will be operated with a Nitronic 50 and Sandvik 2R12 reboiler tube to evaluate fouling tendencies, heat transfer coefficients, and off-gas behavior. Additional operating runs

---

[8]Cartledge, G. H., "Inhibition of Corrosion by the Pertechnetate Ion", Isotope and Irradiation Technology, 1, pp 125-129 (Winter 1963-64).

[9]Coriou, H., Hure, J., and Plante, G., "Electrochemical aspect of the Corrosion of Austenitic Stainless Steel in Nitric Medium and in the Presence of Hexavalent Chromium", Electromchimica Acta, 5, pp 105-11 (1961).

[10]McIntosh, A. B., and Evans, T. E., "The Effect of Metal Species Present in Irradiated Fuel Elements on the Corrosion of Stainless Steel in Nitric Acid", 2nd United Nations Conference on Peaceful Uses of Atomic Energy, Vol. 17 (1958).

[11]Peacock, R. D., The Chemistry of Technetium and Rhenium, New York: American Elsevier, 1966.

will determine corrosion rates for Sandvik 2RE69 and Type 310 stainless steel during the evaporation of simulated HLLW waste solutions. Characterization studies of precipitates and scale deposits will continue. The designing and ordering of construction materials for the small-scale storage tank will be completed.

Laboratory corrosion tests will continue to determine corrosion rates for various rare earth fission products and their substitutes. The effects of technetium and ruthenium will be verified and further investigated.

INTERNAL DISTRIBUTION

1. F. H. Anderson
2. P. A. Anderson
3. J. C. Bishop
4. R. A. Brown
5. B. R. Dickey
6. W. A. Freeby
7. D. A. Knecht
8. H. Lawroski
9. L. C. Lewis
10. F. L. McMillan
11. C. B. Millet
12. B. C. Musgrave
13. B. E. Paige
14. A. P. Roeh
15. K. L. Rohde
16. T. R. Thomas
17. G. R. Villemez
18. B. R. Wheeler
19. M. W. Wilding
20. C. M. Slansky

C. A. Benson (3)
Classification & Technical Information Officer
Idaho Operations Office, ERDA

Chicago Patent Group, ERDA
9800 South Cass Avenue
Argonne, IL 60439

H. P. Pearson, Supervisor
Technical Information
EG&G

INEL Technical Library (10)

EXTERNAL DISTRIBUTION

36. R. C. Adkins, Technical Representative, NUSAC, 777 Leesburg Pike, Falls Church, VA 22043
37. EG&G Idaho, Incorporated, P. O. Box 1625, Idaho Falls, ID 83401
38. H. M. Agnew, Director, Los Alamos Scientific Laboratory, P. O. Box 1663, Los Alamos, NM 87545
39. T. W. Ambrose, Director, Pacific Northwest Laboratory, P. O. Box 999, Richland WA 99352
40. C. K. Anderson, Combustion Engineering Nuclear Power Division, 1000 Prospect Hill Road, Windsor, CT 06095
41. Argonne National Laboratory, P. O. Box 2528, Idaho Falls, ID 83401
42. Argonne National Laboratory, 9700 South Cass Avenue, Argonne, IL 60439
43. J. F. Bader, Manager, Plutonium Recycle Fuel Programs, Westinghouse Electric Corporation, Box 355, Pittsburgh, PA 15230
44. G. W. Cunningham, Division of Nuclear Fuel Cycle and Production, U. S. Energy R&D Administration, Washington, DC 20545
45. Battelle-Columbus Laboratories, 505 King Avenue, Columbus, OH 43201
46. M. Binstock, Kerr-McGee Nuclear Corporation, Kerr-McGee Building, Oklahoma City, OK 73102

47. K. Bowlman, General Electric Company, 175 Curtner Avenue, San Jose, CA 95125
48. R. G. Bradley, Division of Nuclear Fuel Cycle and Production, U.S. Energy R&D Administration, Washington, DC 20545
49. M. G. Britton, Manager Technical Liaison, Corning Glass Works, Corning, NY 14830
50. J. Carp, Director for Energy Policy, Edison Electric, 90 Park Avenue, New York, NY 10016
51. W. T. Cave, Director, Monsanto Research Corporation, Mound Laboratory, P. O. Box 32, Miamisburg, OH 45332
52. B. H. Cherry, Manager of Fuel Resources, GPU Services Corporation, 260 Cherry Hill Road, Parsippany, NJ 07054
53. G. R. Corey, Vice Chairman, Commonwealth Edison Company, P. O. Box 767, Chicago, IL 60690
54. R. G. Cross, DBM Corporation, 1920 Alpine Avenue, Vienna, VA 22180
55. R. Cunningham, Nuclear Materials Safety and Safeguards, Nuclear Regulatory Commission, Washington, DC 20555
56. R. L. Dickeman, President, Exxon Nuclear Company, Inc., 777 106th Avenue, NE, Bellevue, WA 98004
57. Electric Power Research Institute, P. O. Box 10055, Palo Alto, CA 94303
58. R. Fullwood, Science Applications, Inc., 2680 Hanover Street, Palo Alto, CA 94303
59. R. L. Grant, Director of Nuclear Projects, Boeing Engineering and Construction Division, P. O. Box 3707, Seattle, WA 98124
60. Hanford Engineering Development Laboratory, Associate Lab Director, P. O. Box 1970, Richland, WA 99352
61. T. B. Hindman, Jr., Director, Fuel Cycle Project Office, U. S. Energy R&D Administration, Savannah River Operations Office, P. O. Box A, Aiken, SC 29801
62. A. H. Hines, Jr., President, Florida Power Corporation, P. O. Box 14042, St. Petersburg, FL 33733
63. C. A. Hirenda, Director of Marketing, Proposal Management, Inc., 121 N. Orionna Street, Philadelpha, PA 19106
64. P. Hogroian, Division of Nuclear Fuel Cycle and Production, U..S. Energy R&D Administration, Washington, DC 20545
65. R. Hoskins, Tennessee Valley Authority, 217 Electric Power Board Building, Chattanooga, TN 37401
66. C. H. Ice, Director, Savannah River Laboratory, E. I. duPont deNemours and Company, Aiken, SC 29801
67. R. H. Ihde, Manager, Contracts and Marketing, Babcock and Wilcox, P. O. Box 1260, Lynchburg, VA 24505
68. W. Johnson, Vice-President, Yankee Atomic Electric Company, 20 Turnpike Road, Westboro, MA 01581
69. W. A. Kalk, Manager, Nuclear Power Systems, Holmes and Narver, Inc., 400 East Orangethorne Avenue, Anaheim, CA 92801
70. M. I. Kaparstek, Manager of Proposals, Burns and Roe, Industrial Services Corporation, P. O. Box 663, Paramus, NJ 07652
71. K. Killingstad, Cont. Services, Battelle-Human Affairs Research Centers, 4000 N. E. 41st Street, Seattle, WA 98105
72. H. Kouts, Nuclear Regulatory Commission, Washington, DC 20555
73. C. Kuhlman, Division of Nuclear Cycle and Production, U. S. Energy R&D Administration, Washington, DC 20545

74. J. A. Kyger, Associate Director, Argonne National Laboratory, 9700 South Cass Avenue, Argonne, IL 60439
75. F. W. Lewis, President, Middle South Utilities, Inc., Box 61005, New Orleans, LA 70161
76. W. H. Lewis, Nuclear Fuel Services, 6000 Executive Blvd., Rockville, MD 20952
77. J. L. Liverman, Division of Biomedical and Environmental Research, U. S. Energy R&D Administration, Washington, DC 20545
78. H. E. Lyon, Division of Safeguards and Security, U. S. Energy R&D Administration, Washington, DC 20545
79. L. W. Nelms, Chief, Research Branch, Research and Technical Division, Todd Company, P. O. Box 1600, Galveston, TX 77550
80. R. D. Oldenkamp, Rockwell International, Atomics International Division, 8900 De Soto Avenue, Canoga Park, CA 91304
81. G. B. Pleat, Division of Nuclear Fuel Cycle and Production, U. S. Energy R&D Administration, Washington, DC 20545
82. Herman Postma, Director, Oak Ridge National Laboratory, P. O. Box X, Oak Ridge, TN 37830
83. G. K. Rhode, Vice-President-Engineer, Niagara Mohawk Power Corp., 300 Erie Boulevard, West, Syracuse, NY 13202
84. L. M. Richards, Nuclear Commercial Development Coordinator, Atlantic Richfield Company, Box 2679 - TA, Los Angeles, CA 90071
85. R. W. Roberts, Assistant Administrator for Nuclear Energy, U. S. Energy R&D Administration, Washington, DC 20545
86. R. C. Baxter, President, Allied-General Nuclear Services, P. O. Box 847, Barnwell, SC 29812
87. J. Shefcik, General Atomic Company, P. O. Box 81608, San Diego, CA 92138
88. N. F. Seivering, Jr., Assistant Administrator for International Affairs, U. S. Energy R&D Administration, Washington, DC 20545
89. L. E. Smith, Manager-Fuel, Carolina Power and Light Company, P. O. Box 1551, Raleigh, NC 27602
90. D. Spurgeon, Division of Nuclear Fuel Cycle and Production, U. S. Energy R&D Administration, Washington, DC 20545
91. A. Squire, Director, Hanford Engineering Development Laboratory, P. O. Box 1970, Richland, WA 99352
92. C. Stephens, Virginia Electric Power Company, Nuclear Fuel Service Department, 512 Franklin Building, P. O. Box 26666, Richmond, VA 32361.
93. N. Stetson, Manager, U. S. Energy R&D Administration, Savannah River Operations Office, P. O. Box A, Aiken, SC 29810
94. S. Stroller, Western Reprocessors, The S. M. Stoller Corporation, 1250 Broadway, New York, NY 10001
95. K. Street, Associate Director, Lawrence Radiation Laboratory, P. O. Box 808, Livermore, CA 94550
96. G. Stukenbroeker, N. Industries, P. O. Box 928, Barnwell, SC 29812
97. J. D. Tokerud, Vice-President, Aerojet Energy Conversion Company, 1120 Connecticut Avenue, NW, Suite 1050, Washington, DC 20035
98. Dr. Uhrig, Florida Power and Light Company, P. O. Box 013100, Miami FL 33101
99. E. J. Wahlquist, Deputy Assistant Director for Terrestrial Programs, U. S. Energy R&D Administration, Washington, DC 20545
100. W. J. Wilcox, Technical Director, ARGDP, Oak Ridge, TN 27802

101. A. K. Williams, Director, Nuclear Technology Division, Allied-General Nuclear Services, P. O. Box 847, Barnwell, SC 29812
102. U. S. Energy Research & Development Administration, Chicago Operations Office, Contracts Division, 9800 South Cass Avenue, Argonne, IL 60439
103. U. S. Energy R&D Administration, Division of RDD, Energy Systems Analysis, Washington, DC 20545
104. U. S. Energy R&D Administration, Division of RDD, Engineering and Technology, Washington, DC 20545
105. U. S. Energy R&D Administration, Division of RDD, LMFBR Programs, Washington, DC 20545
106. U. S. Energy R&D Administration, Division of RDD, Reactor Safety, Washington, DC 20545
107. U. S. Energy R&D Administration, Library, Washington, DC 20545
108. U. S. Energy R&D Administration, Oak Ridge Operations Office, Manager, P. O. Box E, Oak Ridge, TN 37830
109. U. S. Energy R&D Administration, Oak Ridge Operations Office, Reactor Division, P. O. Box E, Oak Ridge, TN 37830
110. U. S. Energy R&D Administration, Patent Office, Washington, DC 20545
111. U. S. Energy R&D Administration, Richland Operations Office, P. O. Box 550, Richland, WA 99352
112. U. S. Energy R&D Administration, Southern California Energy Program Office, P. O. Box 1446, Canoga Park, CA 91304
113. U. S. Energy R&D Administration, Technical Information Center, Oak Ridge, TN 37820
114. U. S. Energy R&D Administration, Division of Reactor Development Demonstration, Washington, DC 20545
115. U. S. Energy R&D Administration, Idaho Operations Office, 550 Second Street, Idaho Falls, ID 83401
116. U. S. Energy R&D Administration, Nevada Operations Office, P. O. Box 14100, Las Vegas, NV 89114
117. U. S. Energy R&D Administration, San Francisco Operations Office, 1333 Broadway, Wells Fargo Building, Oakland, CA 94612